Published OnlineFirst October 27, 2009; DOI: 10.1158/1078-0432.CCR-09-1315

Mechanisms of Sunitinib Resistance in Gastrointestinal Stromal Tumors Harboring *KIT*$^{AY502-3ins}$ Mutation: An *In vitro* Mutagenesis Screen for Drug Resistance

Tianhua Guo,[1] Mihai Hajdu,[1] Narasimhan P. Agaram,[1] Hiroko Shinoda,[1] Darren Veach,[4] Bayard D. Clarkson,[4] Robert G. Maki,[2] Samuel Singer,[3] Ronald P. DeMatteo,[3] Peter Besmer,[5] and Cristina R. Antonescu[1,5]

Abstract

Purpose: Although tyrosine kinase inhibitors have improved survival in advanced gastrointestinal stromal tumor (GIST), complete response is rare and most patients eventually fail the first-line treatment with imatinib. Sunitinib malate is the only approved second-line therapy for patients with imatinib-resistant or imatinib-intolerant GIST. The clinical benefit of sunitinib is genotype-dependent in regards to both primary and secondary mutations, with GIST patients harboring the *KIT*$^{AY502-3ins}$ exon 9 mutation being the most sensitive.

Experimental Design: As sunitinib resistance is now emerging, our goal was to investigate mechanisms of progression and to test the efficacy of novel tyrosine kinase inhibitor on these resistant mutants *in vitro*. *N*-ethyl-*N*-nitrosourea mutagenesis of Ba/F3 cells expressing the KIT$^{AY502-3ins}$ mutant was used to investigate novel patterns of resistant mutations evolving in the presence of sunitinib.

Results: Tumors from patients who developed sunitinib resistance after at least 1 year of radiographic response were analyzed, showing similar findings of a primary *KIT*$^{AY502-3ins}$ mutation and a secondary mutation in the KIT activation loop. Ba/F3 cells expressing these sunitinib-resistant double mutants showed sensitivity to both dasatinib and nilotinib.

Conclusions: Sunitinib resistance in GIST shares similar pathogenetic mechanisms identified in imatinib failure, with acquisition of secondary mutations in the activation domain after an extended initial response to the drug. Moreover, *in vitro* mutagenesis with or without *N*-ethyl-*N*-nitrosourea of Ba/F3 cells expressing KIT$^{AY502-3ins}$ showed acquisition of secondary mutations restricted to the second kinase domain of KIT. In contrast, *in vitro* resistance to imatinib produces a broader spectrum of secondary mutations including mutations in both KIT kinase domains. (Clin Cancer Res 2009;15(22):6862–70)

Although imatinib achieves a partial response or stable disease in most gastrointestinal stromal tumor (GIST) patients, with lasting responses over 5-year period in >20% of patients, complete responses are rare (1). Clinical responses to imatinib in GIST depend on the presence and type of *KIT* or platelet-derived growth factor receptor-α (*PDGFRA*) gain-of-function mutations. Thus, patients with exon 11 mutations show a partial response rate of 84%, whereas patients with tumors harboring a *KIT* exon 9 or no detectable mutation had a partial response rate of 48% and 0%, respectively (2). It is now clear that a majority of patients who initially benefit from imatinib eventually become resistant. The most common mechanism of acquired resistance is through a secondary *KIT* mutation, usually located in either the NH_2-terminal or the COOH-terminal

Authors' Affiliations: Departments of [1]Pathology, [2]Medicine, and [3]Surgery, Memorial Sloan-Kettering Cancer Center; [4]Molecular Pharmacology and Chemistry Program and [5]Developmental Biology Program, Sloan-Kettering Institute, New York, New York

Received 6/1/09; revised 7/24/09; accepted 8/11/09; published OnlineFirst 10/27/09.

Grant support: ACS MRSG CCE-106841 (C.R. Antonescu), P01CA47179 (C.R. Antonescu, R.G. Maki, and S. Singer), Life Raft Group (C.R. Antonescu and P. Besmer), GIST Cancer Research Fund (C.R. Antonescu and R.P. DeMatteo), Shuman Family Fund for GIST Research (C.R. Antonescu and R.G. Maki), CA102613 (R.P. DeMatteo), CA102774 (P. Besmer), HL/DK55748 (P. Besmer), ARRA CA-198260-01 (R. Maki); NCI-ASCO Cancer Foundation Clinical Investigator Team Leadership Award (R. Maki).

The costs of publication of this article were defrayed in part by the payment of page charges. This article must therefore be hereby marked *advertisement* in accordance with 18 U.S.C. Section 1734 solely to indicate this fact.

Note: Current address for N.P. Agaram: Department of Pathology, Indiana University School of Medicine, Indianapolis, Indiana.

Requests for reprints: Cristina R. Antonescu, Department of Pathology, Memorial Sloan-Kettering Cancer Center, 1275 York Avenue, New York, NY 10021. Phone: 212-639-5721; Fax: 212-717-3203; E-mail: antonesc@mskcc.org.

doi:10.1158/1078-0432.CCR-09-1315

Published OnlineFirst October 27, 2009; DOI: 10.1158/1078-0432.CCR-09-1315

Translational Relevance

Therapy with tyrosine kinase inhibitors (TKI) benefits ~80% of patients with advanced gastrointestinal stromal tumor (GIST), but most patients eventually develop drug resistance. Sunitinib malate is a broad-spectrum TKI approved as second-line therapy for imatinib-resistant GIST patients. The clinical benefit of sunitinib is genotype-dependent, with GIST patients harboring a *KIT* exon 9 mutation being the most sensitive. As sunitinib resistance is now emerging, our goal was to investigate mechanisms of progression and to test the efficacy of novel TKI on these resistant mutants *in vitro*. To establish a comprehensive profile of acquired mutations that confer drug resistance to KIT exon 9 mutants, Ba/F3 cells expressing $KIT^{502\text{-}3AYins}$ were subjected to *N*-ethyl-*N*-nitrosourea mutagenesis and sunitinib selection. The *KIT* mutations identified by *in vitro* screen recapitulated the pattern of second-site mutations observed in TKI-resistant patients. Our findings highlight new mechanisms of resistance to second-generation TKI and provide a preclinical rationale for alternative therapeutic options for patients failing sunitinib therapy.

kinase domain, which disrupts imatinib binding by stabilizing the receptor in a more active conformation. The mechanism for the development of secondary *KIT* mutations remains unclear, but resistant patients with identifiable second-site mutations had been treated with imatinib longer than resistant patients lacking second-site mutations (3). The only Food and Drug Administration–approved second-line tyrosine kinase inhibitor (TKI) for patients with advanced GIST who have progressed on or are intolerant to imatinib is sunitinib malate (Sutent; Pfizer). The clinical benefit from sunitinib following imatinib failure is influenced by the genomic location of both primary and secondary mutations of the activated kinase. Thus, progression-free survival and overall survival are significantly longer for patients with either *KIT* exon 9 mutation or *KIT*/*PDGFRA* wild-type tumors.

Furthermore, imatinib-resistant secondary mutations within the ATP-binding pocket (KIT exons 13 and 14) appear to be sensitive to sunitinib inhibition (4). However, after an initial response, patients developing sunitinib resistance are being diagnosed in the clinic. It remains unclear if similar mechanisms identified in imatinib failure are also responsible for the development of sunitinib resistance. Because sunitinib activity encompasses a broader spectrum of targeted kinases compared with imatinib, including anti–vascular endothelial growth factor receptor activity, it is possible that additional mechanisms play a role in the acquisition of resistance. The goal of our study was first to investigate the clinicopathologic and genomic characteristics associated with patients failing sunitinib therapy. Second, using an *in vitro* model, we tested the efficacy of novel TKI on the sunitinib-resistant mutants. Furthermore, to predict patterns of mutations arising during sunitinib therapy, we used a cell-based screen to identify mutations giving rise to drug resistance, the results of which can be used to generate a genotype-dependent algorithm for drug selection. Using *N*-ethyl-*N*-nitrosourea (ENU), a DNA-alkylating agent that is a highly potent mutagen in mice (5), we established a robust, unbiased mutagenesis system.

ENU mutagenesis alters predominantly AT base pairs and produces A/T->T/A transversions, A/T->G/C transitions, and, with much lower frequency, G/C->A/T transitions, G/C->C/G transversions, A/T->C/G transitions, and % G/C->T/A transitions, thus producing a broad spectrum of missense mutations, which either may be loss-of-function or gain-of-function mutations. ENU mutagenesis was used to compare incidence and types of BCR-ABL kinase domain mutants emerging in the presence of imatinib, dasatinib, and nilotinib alone and in dual combinations in Ba/F3 cells. We have used this approach to investigate the development of drug-resistant mutations in KIT. As the pattern of imatinib-induced resistant mutations has been described in-depth, we focused on identifying mutations conferring sunitinib resistance and acquired secondary mutations associated with $KIT^{502\text{-}3AYins}$ primary mutations. By transforming the Ba/F3 murine pro-B-cell line with $KIT^{502\text{-}3AYins}$, with or without ENU mutagenesis, we were able to reproduce the pattern and relative abundance of sunitinib- and imatinib-resistant secondary mutations identified previously in drug-resistant GIST patients with the exon 9 mutation.

Materials and Methods

Clinicopathologic features. Patients with a diagnosis of GIST, who developed imatinib resistance and subsequently developed progression on sunitinib after at least 1 year on therapy, were identified from our prospective sarcoma database at the Memorial Sloan-Kettering Cancer Center. Those who underwent surgical resection of their resistant tumors were included in the study. Based on the previous experience with imatinib resistance, we selected a 1-year cutoff of clinical response to sunitinib therapy (defined as failure to progress radiographically) to exclude patients with primary resistance and to allow sufficient time for clonal selection of second-site mutations under drug pressure. Clinical information was obtained from the prospective sarcoma database and review of medical charts, including extent of disease at the start of each TKI treatment, duration of imatinib and sunitinib therapy before development of resistance and/or surgical resection, and the best clinical response obtained on each TKI. This study was approved by the institutional review board.

The histologic slides from the surgical specimens were reviewed and the diagnosis of GIST was confirmed based on the morphology and immunostaining for the KIT antibody. Tissue from both imatinib- and sunitinib-resistant GIST resection was available in most cases for analysis of tumor response, such as degree of necrosis, mitotic activity, and expression of KIT.

KIT/PDGFRA *genotyping.* Mutation analysis was done as described previously (6). Genomic DNA was isolated from snap-frozen tumor tissue samples stored at -70°C using a standard phenol-chloroform organic extraction protocol. All cases were tested for the known sites of *KIT* (exons 9, 11, 13, 14, and 17) and *PDGFRA* (exons 12, 14, and 18) mutations. Genomic DNA (1 μg) was subjected to PCR using Platinum TaqDNA Polymerase High Fidelity (Life Technologies). Primer sequences and annealing temperatures were as described (6, 7). Direct sequencing of PCR products was done for all exons tested and each ABI sequence was compared with the National Center for Biotechnology Information human *KIT*and *PDGFRA* gene sequences.

DNA constructs. The retroviral vector plasmid containing wild-type human *KIT* cDNA (GNNK- isoform), pMSCV-WT*KIT*-IRES-GFP, was generously provided by Dr. Gary Gilliland (Harvard Medical School). *KIT* mutations recapitulating the genotype found in sunitinib

Published OnlineFirst October 27, 2009; DOI: 10.1158/1078-0432.CCR-09-1315

malate-resistant GIST patients were generated by site-directed mutagenesis PCR using QuikChange II XL Site-Directed Mutagenesis kit (Qiagen). *KIT* double-mutant isoforms hosting primary exon 9 mutation and an acquired secondary mutations in exon 13 or 17 were generated as follows: $KIT^{502\text{-}3AYins/V654A}$, $KIT^{502\text{-}3AYins/D820Y}$, and $KIT^{503\text{-}3AYins/N822K}$. $KIT^{502\text{-}3AYins}$ single mutant was used as a control. All constructs were verified with direct sequencing.

Establishing Ba/F3* KIT *mutants stable transformant cell lines. The interleukin-3–dependent Ba/F3 murine pro-B cell line was obtained from the German Collection of Microorganisms and Cell Culture. Ba/F3 cells were transfected and selected as described previously (8). Briefly, Ba/F3 cells were cotransfected with retroviral vector plasmids containing *KIT* cDNA mutant isoforms and linear hygromycin-resistant DNA via electroporation. The electroporated cells were first grown in the presence of hygromycin for 10 days followed by sorting according to green fluorescent protein. Green fluorescent protein–positive cells were further grown for another 2 weeks in the presence of interleukin-3 and then transformed to interleukin-3–independent on interleukin-3 withdrawal. Ba/F3 $KIT^{502\text{-}3AYins}$ cells were supplemented with 20 ng/mL KIT ligand; all the double mutants described above did not require KIT ligand supplement. Cells were stained with PE-conjugated anti-CD117 antibody (BD Biosciences) and monitored by flow cytometry. Cell lysates were subjected to Western blotting using anti-KIT antibody (Calbiochem).

Inhibitors and* in vitro *drug testing. The following TKI were used: imatinib, sunitinib, sorafenib, dasatinib, and nilotinib. Nilotinib and dasatinib were synthesized in-house and kindly provided by Dr. Bayard Clarkson's laboratory at Memorial Sloan-Kettering Cancer Center. Imatinib, sunitinib, and sorafenib were purchased commercially and purified with column chromatography by Dr. Bayard Clarkson's laboratory at Memorial Sloan-Kettering Cancer Center. The kinases inhibitors were dissolved at 10 mmol/L in DMSO as stocks and working dilutions were freshly made before experiments.

Cell proliferation assays. Ba/F3 cells (0.5×10^5 per well) expressing KIT mutants were incubated with 10, 100, 1,000, 5,000, and 10,000 nmol/L imatinib, sunitinib, nilotinib, dasatinib, and sorafenib in 96-well plates at 37°C for 48 h in triplicate. Cells were incubated for 4 h with [^{3}H]thymidine (1 μCi; 0.037 MBq) before harvesting and [^{3}H]thymidine incorporation was determined. Growth inhibition was plotted as the ratio of the average [^{3}H]thymidine incorporation in drug-treated wells relative to no-drug controls. IC_{50} values for tested inhibitors were calculated by GraphPad Prism software version 5.00.

Apoptosis assays. Cells at a density of 1×10^6 were cultured in 24-well plates and incubated with imatinib, sunitinib, nilotinib, dasatinib, and sorafenib at concentrations to a range of 10, 100, 1,000, and 5,000 nmol/L for 48 h. Cells were harvested and stained with anti–Annexin V-PE antibody and 7-amino-actinomycin D (BD Biosciences). A minimum of 20,000 events were analyzed by FACScan (Becton Dickinson) within 1 h after staining. Data were analyzed by FlowJo 7.1.3.

Immunoprecipitation and Western blotting. Ba/F3 cells expressing KIT mutant isoforms were starved from serum and treated with the indicated concentrations of each inhibitor for 90 min. Cell lysis, immunoprecipitations, and immunoblotting were done as described previously (8). Cell lysates were incubated with anti-KIT antibody (Assay Designs) and Magna beads (Pierce Biotechnology) overnight at 4°C. The precipitated KIT was separated by electrophoresis and transferred to nitrocellulose. Blots were probed with anti-phospho-tyrosine anti-bodies PY20 and PY99 (Santa Cruz Biotechnology), stripped, and reprobed with rabbit polyclonal anti-KIT antibody (Calbiochem).

ENU mutagenesis. Ba/F3 $KIT^{502\text{-}3AYins}$ cells were maintained in complete culture medium, RPMI 1640 containing 10% serum, 1% penicillin/streptomycin, and 20 ng/mL KIT ligand at an exponential growth rate. Cells were incubated with ENU (50 μg/mL) at a density of 5×10^6/mL for 24 h and then washed three times with RPMI 1640, replated in complete medium, and expanded for 1 week under exponential growth conditions.

In vitro mutagenesis screen. ENU-exposed Ba/F3 $KIT^{502\text{-}3AYins}$ cells were cultured in 96-well plates (1.0×10^5 per well) in 150 μL complete medium in the presence of various concentrations of sunitinib and imatinib. Sunitinib was supplemented at 0.05, 0.1, 0.25, 0.5, and 1 μmol/L, and imatinib at 0.5, 1, 2.5, 5, and 10 μmol/L, which corresponded to 1, 2, 5, 10, and 20 times their IC_{50} values (sunitinib = 54 nmol/L and

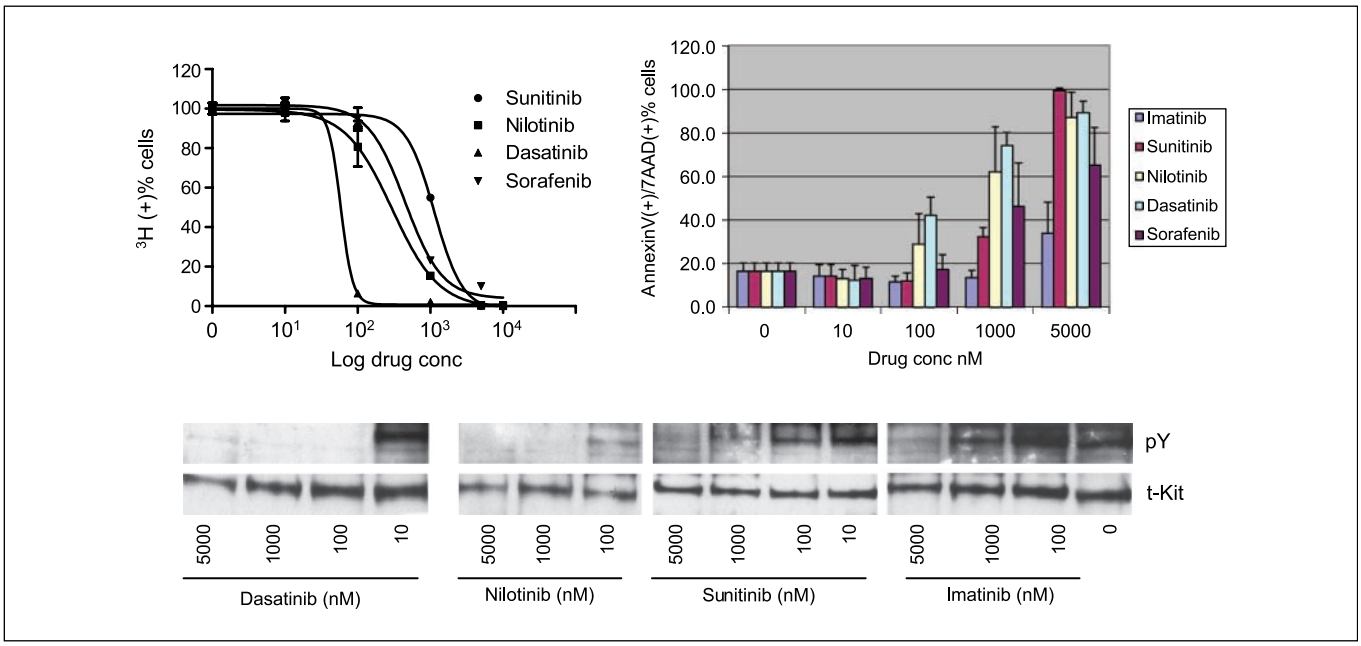

Fig. 1. Imatinib-resistant Ba/F3 $KIT^{502\text{-}3AYins/D820Y}$ double mutant is sensitive to dasatinib and nilotinib inhibition but insensitive to sunitinib and imatinib. Dasatinib and nilotinib remarkably abolished the mutant KIT kinase activity at 100 and 1,000 nmol/L and inhibited cell growth with IC_{50} values of 40.6 and 248 nmol/L, respectively. Both drugs induced >50% of apoptosis at 1,000 nmol/L. Sunitinib- and imatinib-treated cells showed reduced KIT kinase activity at 1,000 and 5,000 nmol/L, respectively. Sunitinib inhibited cell proliferation with an IC_{50} of 1,486 nmol/L and induced significant apoptosis at 5,000 nmol/L. In contrast, imatinib did not show growth inhibition or induce apoptosis up to 5,000 nmol/L. Sorafenib inhibited cell proliferation with an IC_{50} of 842 nmol/L and induced moderate apoptosis at 500 nmol/L.

Published OnlineFirst October 27, 2009; DOI: 10.1158/1078-0432.CCR-09-1315

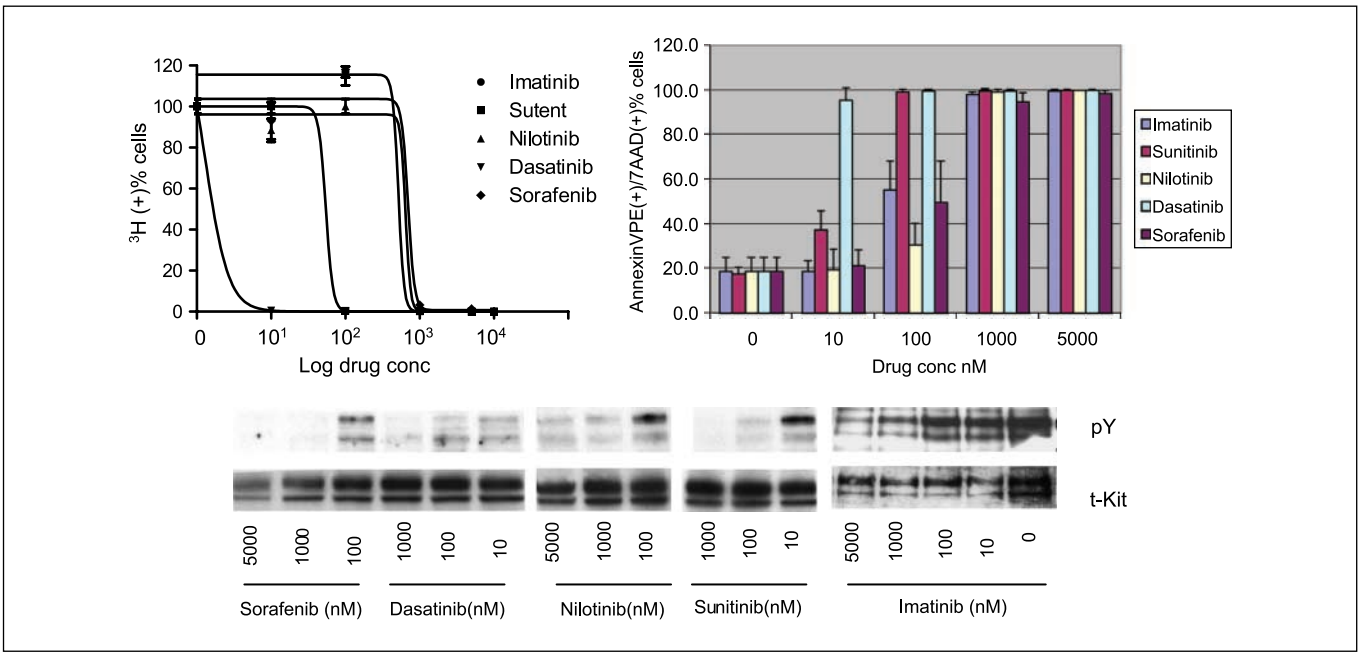

Fig. 2. *In vitro* drug sensitivity of Ba/F3 KIT$^{502\text{-}3AYins}$ single mutant. Sunitinib and dasatinib inhibited KIT kinase activity at ≤10 nmol/L, inhibited cell proliferation with IC_{50} values of 54 and 2.9 nmol/L, and induced significant apoptosis at 100 and 10 nmol/L, respectively. Imatinib, nilotinib, and sorafenib inhibited KIT phosphorylation between 100 and 1,000 nmol/L, inhibited cell growth with IC_{50} values of 517, 695, and 861 nmol/L, respectively, and induced significant apoptosis at 1,000 nmol/L.

imatinib = 517 nmol/L), respectively. The number of resistant colonies was counted by visual inspection every 2 to 3 days for at least 4 to 6 weeks. Single colonies were picked and expanded for analysis in 1 mL complete medium in the presence of the corresponding concentration of inhibitors used in the screen. Genomic DNA was extracted and subjected to PCR for possible mutations in the main hotspots (*KIT* exons 13, 14, and 17; ref. 3). In parallel, Ba/F3 *KIT*$^{AY502\text{-}3ins}$ cells without ENU exposure were incubated with the same concentrations for each inhibitor. Resistant colonies were inspected and analyzed with the same protocol as the ENU-exposed cells. Ba/F3 *KIT*$^{WK557\text{-}8del}$ cells with or without ENU treatment were grown in complete medium supplemented with 0.05, 0.1, 0.25, 0.5, and 1.0 μmol/L imatinib according to 1, 2, 5, 10, and 20 times its IC_{50}, respectively. Resistant colony selection and analysis were conducted as described above as an isoform control.

Fluorescence* in situ *hybridization. Cells were treated with colcemid (Life Technologies) at 50 ng/mL for 45 min before harvesting. *KIT*$^{AY502\text{-}3ins}$ DNA was labeled with digoxingenin-11-dUTP (Roche) by nick translation. The slides and the probes were codenatured at 70°C for 5 min and then incubated at 37°C overnight in a dark moist chamber. Posthybridization wash was carried at 45°C with 50% formamide/2× SSC. Mouse anti-digoxigenin IgG (5 μg/mL; Roche) and FITC-conjugated goat anti-mouse IgG (5 μg/mL; Invitrogen) were used for detection. The cells were then stained with 4′,6-diamidino-2-phenylindole (Molecular Probes). Slides were viewed with a Nikon E600 epifluorescence microscope.

Results

Secondary KIT mutations in the activation loop are associated with sunitinib resistance. We identified three imatinib-resistant patients who showed a clinical response to sunitinib for >1 year (mean, 23 months) before progressing and subsequently referred for surgical management. Tissue from the sunitinib-resistant nodules was available for genotyping. The sunitinib-resistant patients shared similar clinicopathologic and molecular findings: all had their primary GIST located in the small bowel, harbored a primary *KIT* exon 9 mutation, and showed a partial response to imatinib therapy for a mean of 24 months (range, 18-28) before developing progression. Furthermore, both patients with tissue available before sunitinib therapy lacked second-site imatinib-resistant mutations.

On microscopic evaluation, all sunitinib-resistant tumors showed increased cellularity, brisk mitotic activity, and strong and diffuse KIT immunoreactivity. The genotype analysis of the eight nodules from the three sunitinib-resistant patients revealed three different amino acid substitutions in the KIT activation loop (exon 17): *D820Y*, *D820E*, and *N822K*. In one patient, only one of the six resistant nodules analyzed showed the presence of a second-site *KIT* mutation (*D820E*).

Ba/F3 cells expressing KIT exon 9/exon 17 double mutants are sensitive to dasatinib and nilotinib inhibition. To investigate the sensitivity of sunitinib-resistant KIT mutants to other TKIs, we established stable Ba/F3 cell lines expressing primary *KIT* exon 9 (*KIT*$^{502\text{-}3AYins}$) and secondary mutations in *KIT* exon 13 (*KIT*^{V654A}) and exon 17 (*KIT*^{D820Y}, *KIT*^{N822K}). *KIT*$^{502\text{-}3AYins/D820Y}$ and *KIT*$^{502\text{-}3AYins/N822K}$ were identified in sunitinib-resistant GIST patients. The third secondary mutation identified in a sunitinib-resistant patient, exon 17 *KIT*^{D820E}, failed transfection. The *KIT*$^{502\text{-}3AYins/V654A}$ mutant described previously in an imatinib-resistant, sunitinib-sensitive patient (4) was used as a control.

The efficacy of five TKIs with anti-KIT activity, including imatinib, sunitinib, nilotinib, dasatinib, and sorafenib, was tested in Ba/F3 *KIT* transfectants expressing the sunitinib-resistant double mutants, *KIT*$^{502\text{-}3AYins/D820Y}$ and *KIT*$^{502\text{-}3AYins/N822K}$, recapitulating mutations identified in patients, and compared with the imatinib- and sunitinib-sensitive KIT ectodomain mutant, *KIT*$^{502\text{-}3AYins}$, as well as to the imatinib-resistant and sunitinib-sensitive double mutant, *KIT*$^{502\text{-}3AYins/V654A}$. Each cell line was treated with similar escalating doses of the five inhibitors.

Published OnlineFirst October 27, 2009; DOI: 10.1158/1078-0432.CCR-09-1315

Inhibition of KIT kinase activity was monitored by immunoblotting and the biological consequences were evaluated by determining proliferation inhibition and induction of apoptosis. Growth-inhibitory effects were determined by ^{3}H incorporation, whereas induction of apoptosis was evaluated by flow cytometry using Annexin V-PE Apoptosis Detection kit (Pharmingen).

Ba/F3 cells expressing exon 17 secondary mutations, *KIT*$^{502\text{-}3AYins/D820Y}$, were resistant to either imatinib or sunitinib inhibition. Imatinib did not inhibit KIT phosphorylation at concentrations <5,000 nmol/L, nor did it show effects in biological assays. Sunitinib did not show any cellular effects <1,000 nmol/L, inhibiting cell growth with an IC_{50} of 1,486 nmol/L and inducing mild apoptosis at 1,000 nmol/L (Fig. 1), although it abrogated KIT kinase activity between 100 and 1,000 nmol/L. However, dasatinib completely abolished KIT phosphorylation at a low dose (10-100 nmol/L). Dasatinib also showed an excellent efficacy inhibiting cell growth, with an IC_{50} of 40.6 nmol/L and inducing apoptosis between 100 and 1,000 nmol/L. Nilotinib treatment resulted in marked decrease of KIT kinase activity <100 nmol/L and showed potent proliferation inhibition with an IC_{50} of 248 nmol/L. Induction of apoptosis was achieved with a higher dose of nilotinib (1,000 nmol/L; Fig. 1).

Similar experiments were done with Ba/F3 cells expressing the *KIT*$^{502\text{-}3AYins/N822K}$ mutant resulting in a comparable drug sensitivity profile. Although imatinib and sunitinib partially inhibited KIT kinase activity of this double mutant, cell proliferation or induction of apoptosis was not affected <1,000 nmol/L. In contrast, dasatinib and nilotinib inhibited the kinase activity at concentrations <100 and 1,000 nmol/L, inhibited cell growth with an IC_{50} values of 66.2 and 309 nmol/L, and induced apoptosis at 100 and 1,000 nmol/L, respectively. In contrast, Ba/F3 *KIT*$^{502\text{-}3AYins}$ cells were highly sensitive to both dasatinib and sunitinib and less sensitive to imatinib and nilotinib inhibition. Dasatinib and sunitinib inhibited cell growth with IC_{50} of 2.9 and 54 nmol/L, respectively. Dasatinib induced significant apoptosis at 10 nmol/L, whereas sunitinib induced apoptosis between 10 and 100 nmol/L. Furthermore, dasatinib dramatically decreased KIT kinase autophosphorylation at <10 nmol/L, whereas sunitinib showed marked inhibition of KIT kinase autophosphorylation between 10 and 100 nmol/L. Imatinib produced moderate inhibition on KIT kinase activity at 1,000 nmol/L, with an IC_{50} of 517 nmol/L, whereas nilotinib and sorafenib inhibited kinase activity at 100 nmol/L, with IC_{50} values of 695 and 861 nmol/L, respectively. These three inhibitors induced significant apoptosis at 1,000 nmol/L (Fig. 2).

As noted previously in the imatinib-resistant patients (9), our *in vitro* results validate that the secondary mutations in the ATP-binding pocket remain sensitive to sunitinib inhibition. Inhibition of KIT activation of the Ba/F3 *KIT*$^{502\text{-}3AYins/V654A}$ double-mutant was achieved with <10 nmol/L sunitinib, whereas inhibition of cell proliferation with an IC_{50} of 20.6 nmol/L, concomitant with induction of apoptosis at 100 nmol/L. Dasatinib-treated cells also showed dramatic decrease of KIT kinase activity at 10 nmol/L, whereas the IC_{50} for proliferation was 334.5 nmol/L and at 1,000 nmol/L induction of apoptosis ~70%. Imatinib partially inhibited KIT phosphorylation at 1,000 nmol/L but did not arrest the growth or induce apoptosis <5,000 nmol/L compared with the untreated control. Although nilotinib showed overt inhibition on KIT phosphorylation at 1,000 nmol/L and an IC_{50} of 1,045 nmol/L with regards to inhibition of cell proliferation, it did not induce apoptosis at a comparable dose. Table 1 summarizes these results in comparison with the IC_{50} of Ba/F3 KIT double mutants carrying a KIT exon 11 primary mutation (published in ref. 8).

Sorafenib showed moderate inhibition on KIT*$^{502\text{-}3AYins}$ *single mutant but only mild efficacy on KIT*$^{502\text{-}3AYins}$ *double mutants. In Ba/F3 cells expressing *KIT*$^{502\text{-}3AYins}$, sorafenib inhibited the mutant kinase at 100 to 1,000 nmol/L, induced moderate apoptosis at 100 nmol/L, and inhibited cell proliferation with an IC_{50} of 861 nmol/L. In contrast, it inhibited exon 9 double mutants, *KIT*$^{502\text{-}3AYins/D820Y}$, *KIT*$^{502\text{-}3AYins/N822K}$, and *KIT*$^{502\text{-}3AYins/V654A}$, with IC_{50} values of 842, 933, and 1,672 nmol/L, respectively, but did not induce significant apoptosis at comparable doses.

In vitro *screen for sunitinib resistance revealed second-site mutations in the activation loop of KIT.* To investigate the mechanisms of sunitinib resistance and generate a comprehensive map of acquired mutations, we developed a cell-based screen for drug resistance of *KIT*$^{502\text{-}3AYins}$-associated secondary mutations. Ba/F3 *KIT*$^{502\text{-}3AYins}$ cells were treated with the mutagen ENU. Subsequently, the ENU-treated Ba/F3 *KIT*$^{502\text{-}3AYins}$ cells were incubated with sunitinib or imatinib to identify drug-resistant colonies. The incidence, patterns, and types of mutations acquired by sunitinib selection were compared with the ones induced by imatinib treatment. Furthermore, non-ENU-exposed Ba/F3 *KIT*$^{502\text{-}3AYins}$ cells were selected with the identical doses of sunitinib and imatinib to compare the resistance frequencies and mutation spectrum. To exclude the possibility that resistant colonies develop intrinsically due to genetic instability, Ba/F3 *KIT*$^{502\text{-}3AYins}$ cells were also screened without inhibitors. Cells cultured with KIT ligand, KITL, supplemented in the absence of TKI grew back in a week, without finding secondary mutations in randomly tested cells.

In concordance with the sunitinib-resistant genotypes observed in patients, the cell-based mutagenesis also showed that acquired secondary mutations in Ba/F3 *KIT*$^{502\text{-}3AYins}$ cells were only found in the KIT activation loop. Sequencing of 100 sunitinib-resistant clones resulting from the ENU-treated Ba/F3 *KIT*$^{502\text{-}3AYins}$ cells and 117 clones from the untreated cells showed that all secondary mutations are single amino acid substitutions in *KIT* exon 17, including *D816V*, *D816F*, *D816A*, *D816H*, *D816Y*, and *D820G* (Fig. 3). Among these mutations, *D816V* was the most prevalent substitution, accounting for 6.7% of ENU-treated resistant colonies. ENU-mutagenesis did not generate distinct

Table 1. Comparative efficacy of TKI in BA/F3 KIT double mutants, harboring either a KIT exon 9 or exon 11 primary mutation

Mutations	IC_{50} (nmol/L)		
	Nilotinib	Dasatinib	Sorafenib
KIT$^{502\text{-}503AY/V654A}$	1,045	334.5	1,672
KIT$^{V560del/V654A}$	192	585	1,074
KIT$^{502\text{-}503AY/D820Y}$	248	40.6	842
KIT$^{V559D/D820Y}$	297	432	944
KIT$^{502\text{-}503AY/N822K}$	369	66.2	933
KIT$^{V560del/N822K}$	NA	NA	NA

Published OnlineFirst October 27, 2009; DOI: 10.1158/1078-0432.CCR-09-1315

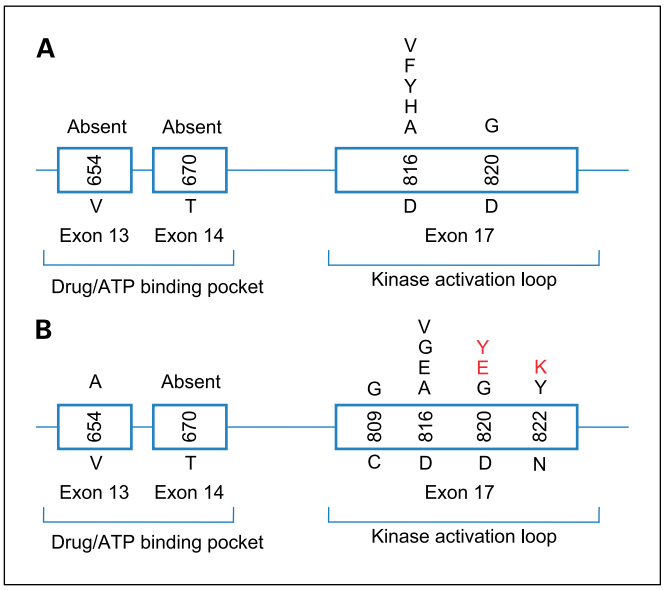

Fig. 3. Distribution of point mutations in a cell-based screen for sunitinib resistance of BaF3 KIT$^{AY502-3ins}$ cells compared with the genotype in sunitinib- and imatinib-resistant patients. *A,* secondary mutations identified under the sunitinib screen were restricted to the KIT activation loop, being single amino acid substitutions at positions of D816 and D820. *B,* secondary mutations identified in sunitinib-resistant patients (*red font*) were limited to the activation loop in the COOH-terminal kinase domain of KIT protein, and imatinib-resistant patients (*black*) with a primary KIT exon 9 mutation were located in both ATP-binding and catalytic domains, with a similar amino acid substitution pattern (3, 9, 24).

secondary mutations compared with the non-ENU group. However, the spectrum of sunitinib-resistant mutations was more limited compared with the imatinib selected screen. Sequencing of 78 clones obtained after ENU treatment and 158 clones from non-ENU Ba/F3 *KIT*$^{502-3AYins}$ cells, imatinib-resistant mutations were observed in both KIT kinase domains, including *T670I*, *D816V*, and *D816F*.

The incidence of each type of mutation identified in sunitinib-resistant clones emerging from Ba/F3 *KIT*$^{502-3AYins}$ cells varied from 1% to 14% according to different doses (Fig. 4A), with overall mutation rates of 3.3%, 9.5%, and 5.6% at 2, 5, and 10 times IC_{50}. The rate of imatinib-resistant clones under similar conditions was higher (19.4%, 8%, and 67%, respectively). The resistant mutations were limited to D816V at higher doses (10 times IC_{50}) for both inhibitors tested. At >20 times IC_{50}, both drugs sufficiently suppressed the emergence of resistant colonies.

In contrast, the mutation rates of imatinib-resistant clones selected by similar dosages in Ba/F3 *KIT*$^{557-8WKdel}$ cells were ~90% regardless of ENU treatment, displaying a similar mutation spectrum, including *D816V*, *D816Y*, *N822K*, *N655K*, and *T670I* (data not shown). The most prevalent mutation remained at D816, *D816V* with ENU treatment (79%) and *D816Y* in the non-ENU group (86.5%).

Frequency of resistant clones increased with ENU exposure and lower concentration of inhibitors. To determine whether the induced drug resistance was dose-dependent, ENU-treated Ba/F3 *KIT*$^{502-3AYins}$ cells were exposed to escalating concentrations of sunitinib (0.05, 0.1, 0.25, 0.5, and 1 μmol/L corresponding to 1, 2, 5, 10, and 20 times IC_{50}, respectively). Non-ENU-treated Ba/F3 *KIT*$^{502-3AYins}$ cells were treated with similar doses of sunitinib and imatinib. The frequencies of resistant colonies were determined by visual inspection of the number of colonies relative to the total number of cells. The frequency of resistant colonies decreased with increasing sunitinib dose, with a rate of 6.8×10^{-6}, 6.7×10^{-6}, 5.4×10^{-6}, 2.2×10^{-6}, and 0.35×10^{-6} at 1, 2, 5, 10, and 20 times IC_{50}, respectively (Fig. 4B). Imatinib selected colonies of ENU-treated Ba/F3 *KIT*$^{502-3AYins}$ cells showed similar dose-dependent resistant frequencies of 10×10^{-6}, 5.8×10^{-6}, 2.9×10^{-6}, 0.35×10^{-6}, and 0.1×10^{-6} at similar doses.

Cells exposed to lower doses than the IC_{50} of sunitinib (10 and 20 nmol/L) grew back without individual colony formation within a week, suggesting that these concentrations did not sufficiently inhibit Ba/F3 *KIT*$^{502-3AYins}$ cells. Conversely, at >20 times the IC_{50} of sunitinib, no resistant colonies evolved within 60 days. Similar observations were made with imatinib.

Untreated Ba/F3 *KIT*$^{502-3AYins}$ cells yielded a lower frequency of resistant colonies compared with ENU-treated cells at similar drug concentrations ($P < 0.01$, pair of comparison χ^2). The frequency of resistant colonies observed in non-ENU conditions was 1.4, 1.15, 0.8, 0.4, and 0 colonies per million cells at 1, 2, 5, 10, and 20 times IC_{50} of sunitinib, respectively (Fig. 4B). The incidence of imatinib-resistant colonies in non-ENU-treated group was 5.1, 3.1, 1.45, 0.05, and 0 colonies per million cells at equipotent dosages. No overt difference in the median growth time of resistant colonies was seen between sunitinib- and imatinib-selected BaF3 *KIT*$^{502-3AYins}$ cells.

Sunitinib-selected resistant clones were insensitive to sunitinib and imatinib inhibition. To validate that clones derived from the sunitinib-resistant screen were indeed refractory to sunitinib inhibition, cells were cultured in the presence of various concentrations of sunitinib, and IC_{50} values were determined. In parallel, the imatinib IC_{50} values was also determined in these cells. Sunitinib-selected clones, with or without secondary mutations, were tested, showing similar insensitivity to sunitinib compared with sunitinib-sensitive parental Ba/F3 KIT$^{AY502-3ins}$ cells. The imatinib IC_{50} values in these clones was >5 μmol/L.

KIT$^{AY502-3ins}$ sunitinib-resistant clones show biochemical activation of KIT but no alteration in KIT copy number. By Western blot, protein extracts from KIT$^{AY502-3ins}$-resistant clones showed similar levels of total and phosphorylated KIT expression to the parental sunitinib-sensitive Ba/F3-KIT$^{AY502-3ins}$ cells. To explore the possibility of *KIT* copy number changes in sunitinib-resistant clones without detectable secondary mutations, we investigated the genomic integration of KIT$^{AY502-3-ins}$ cDNA plasmid in both parental Ba/F3 KIT$^{AY502-3ins}$ and sunitinib-resistant clones. Cells were subjected to fluorescence *in situ* hybridization using digoxigenin-labeled KIT$^{AY502-3ins}$ cDNA, showing a single integration site on chromosome 6C2 in both groups. Therefore, no genetic difference related to the KIT locus was noted between the parental Ba/F3 KIT$^{AY502-3-ins}$ and the sunitinib-resistant clones.

Discussion

The primary genetic event responsible for the pathogenesis of GIST is a gain-of-function mutation in the *KIT* proto-oncogene or, less commonly, in the *PDGFRA* gene (10, 11). More than two-thirds of all GIST patients carry mutations in *KIT* exon 11, which encodes the juxtamembrane domain, whereas ~10% to 15% of patients show mutations within the extracellular domain of KIT (in exon 9; refs. 6, 12). The vast majority of *KIT* exon 9 mutations represent an identical tandem duplication of

Published OnlineFirst October 27, 2009; DOI: 10.1158/1078-0432.CCR-09-1315

six nucleotides, encoding AY 502-503. GISTs harboring *KIT* exon 9 mutations define a distinct subset, characterized predominantly by small bowel location and an aggressive clinical behavior (6, 13).

Therapeutic inhibition of KIT and PDGFRA kinase activity by imatinib mesylate (Gleevec; Novartis) has emerged as frontline treatment for patients with metastatic or locally advanced inoperable GIST. Imatinib achieves disease control in 70% to 85% of patients with advanced GIST. The clinical response varies significantly according to different molecular subtypes of GIST. As such, patients with GIST carrying *KIT* exon 11 mutations show the best response to imatinib with a partial response rate of 84% compared with only 48% in patients with *KIT* exon 9 mutations (2). *KIT* exon 9 mutations were the strongest adverse prognostic indicator for response to imatinib, increasing the relative risk of progression by 171% and the relative risk of death by 190% (14). Furthermore, patients whose tumors harbored *KIT* exon 9 mutations had a significantly superior progression-free survival when treated with the high-dose regimen compared with patients with exon 11 mutations (14). However, in spite of the prolonged responses with escalating imatinib dose, most patients subsequently experienced disease progression.

The only Food and Drug Administration–approved second-line TKI for patients with advanced GIST, who have progressed on or are intolerant of imatinib, is sunitinib malate. Sunitinib is a small-molecule TKI with potent antiangiogenic and antitumor activities, which has shown efficacy against GIST, acceptable tolerability, and safety in a double-blind placebo-controlled phase III trial (15). Patients with *KIT* exon 9 mutations GISTs showed the most sustained response to sunitinib inhibition. As sunitinib resistance is now emerging in the clinical practice, new therapeutic strategies are needed to treat these patients.

As learned from the imatinib resistance experience, second-site *KIT* mutations develop more frequently in association with primary *KIT* exon 11 mutations, which confer the most sustained clinical response to imatinib. This finding might reflect the long time-span of exposure to the drug and not only due to the location of the primary mutations. Thus, secondary mutations were found in 73% to 86% of imatinib-resistant patients harboring exon 11 primary mutations and only 19% to 33% of patients with exon 9 primary mutation developed secondary mutations (3, 9, 16). Furthermore, the pattern of the second-site mutations in the setting of imatinib resistance was exclusively point mutations, evenly divided between the first and the second kinase domains (3, 17, 18). In keeping with these observations, the three patients who developed sunitinib resistance after at least 1 year of clinical benefit had second-site mutations in the KIT kinase activation domain (*N822K*, *D820Y*, and *D820E*). Expression of these sunitinib-resistant double mutants in an *in vitro* Ba/F3 model showed sensitivity to both dasatinib and nilotinib, suggesting alternative therapeutic options for these patients.

To establish a comprehensive profile of acquired secondary mutations that confer drug resistance to KIT exon 9 mutants, Ba/F3 cells expressing $KIT^{502\text{-}3AYins}$ were subjected to ENU mutagenesis followed by sunitinib selection and emerging resistant clones were identified and characterized. The KIT mutations identified by *in vitro* mutagenesis recapitulated the type and location of second-site *KIT* mutations observed in both sunitinib- and imatinib-resistant patients. Thus, all sunitinib-resistant secondary mutations identified in the Ba/F3-$KIT^{502\text{-}3AYins}$ cells were similarly point mutations in the KIT kinase activation loop. However, the mutations identified in the *in vitro* screen were dominated by *D816V*. The high incidence of this mutation is most likely conferred by the significant advantage in its activation rate. Substitutions at this site, *D816H/V*, have shown increases in activation rate of 184- and 536-fold, respectively (19). Furthermore, D816 mutations appear to negatively influence the inhibitory conformation of the juxtamembrane domain of KIT (19). Several substitutions at this site have been described in TKI-resistant GIST patients, including D816H/F/A/G/E/V. However, the rarity of *D816V* mutation in progressing GIST patients might be an indication of its high malignancy, which may induce tumor lethality *in vivo*. Alternatively, the possibility of this dominant D816V genotype being intrinsic to the Ba/F3 cells system remains a consideration, because Ba/F3 cells are

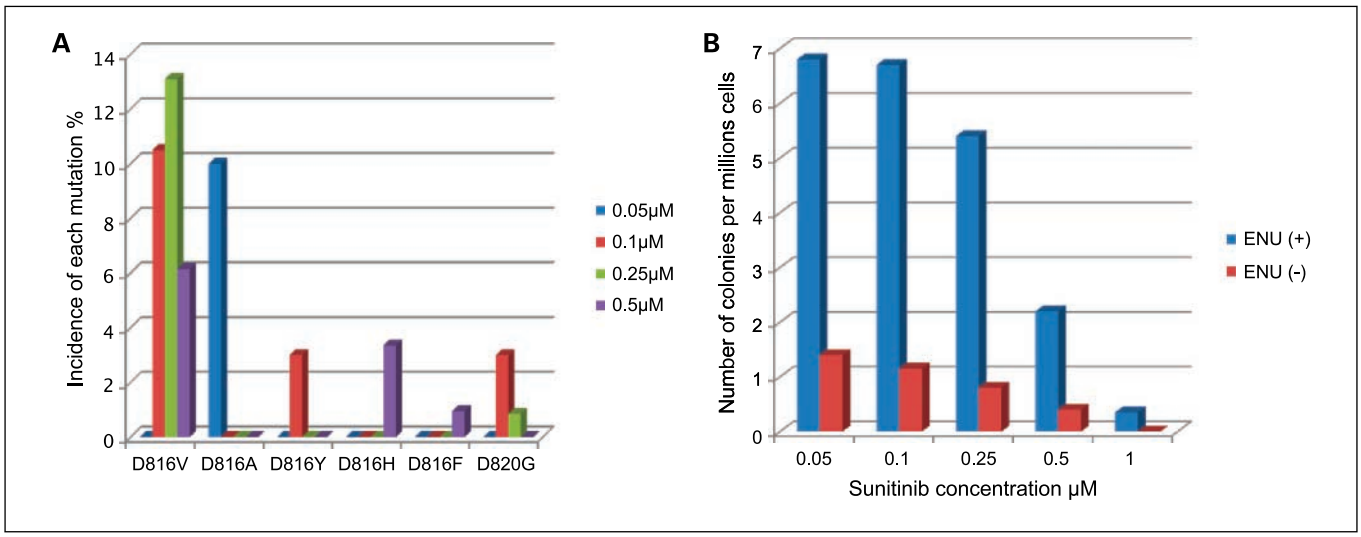

Fig. 4. Spectrum of acquired secondary mutations and frequency of resistant colonies in cell-based screen for sunitinib resistance. *A*, spectrum of secondary mutations was dominated by *D816V* followed by *D816A*. Other substitutions seen at a similar lower rate included *D816F*, *D816H*, *D816Y*, and *D820G*. *B*, frequency of resistant colonies was dose-dependent and higher in ENU-exposed Ba/F3 $KIT^{AY502\text{-}3ins}$ cells. Escalating doses reduced the incidence of resistant colonies. Exposure to ENU mutagen significantly increased the frequency of resistant colonies.

Published OnlineFirst October 27, 2009; DOI: 10.1158/1078-0432.CCR-09-1315

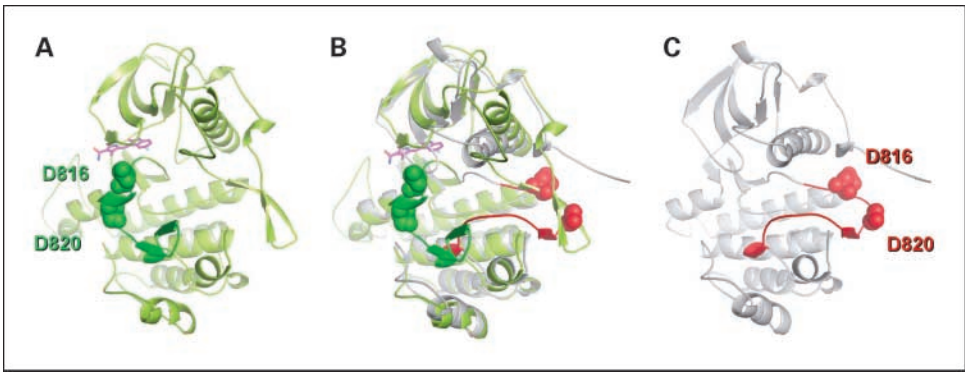

Fig. 5. Comparison of the structures of the inactive KIT kinase in complex with sunitinib and the activated KIT kinase. *A,* inactive kinase shown in light green, activation loop in green, and sunitinib in magenta. *B,* superposition of the inactive (*A*) and the active (*C*) kinase structures. *C,* structure of the activated KIT kinase is shown in gray and the activation loop in red. The position of second-site mutation in the activation loop, D816 and D820, are indicated. Adapted from ref. 19.

murine pro-B cells and *D816V* is the common mutation in mastocytosis.

Importantly, *KIT* exon 13 and 14 mutations were not detected either in the sunitinib resistance screen or in progressing tumors of patients of sunitinib-resistant patients, as sunitinib is known to be efficacious with ATP-pocket second-site mutations (4, 9). In contrast, *in vitro* mutagenesis of Ba/F3 KIT$^{502\text{-}3AYins}$ cells and selection with imatinib identified secondary mutations mapped in both KIT kinase domains (mostly *D816V* and *T670I*). These findings are in agreement with results of *in vitro* mutagenesis of Ba/F3 Bcr-Abl cells, in which the vast majority of imatinib-resistant mutations were substitutions within the kinase domain of the fusion protein (20, 21). However, the spectrum of resistance mutations obtained with Ba/F3 KIT$^{502\text{-}3AYins}$ cells was narrower compared with the results obtained with Bcr-Abl. The observed difference most likely is not related to the methodology used, which was very similar in both studies but rather intrinsic to the specific oncogenes tested. The relatively limited variety of mutations observed in the Ba/F3 KIT$^{502\text{-}3AYins}$ screen cannot be explained only by the lower rate of mutation detected in the resistant clones, because a significantly higher rate of mutations (90%) noted in the Ba/F3-KIT$^{557\text{-}8WKdel}$ cells was not accompanied by an enhanced mutation spectrum. To overcome the low yield of resistant colonies, ENU mutagenesis was applied, which indeed increased the frequency of both sunitinib- and imatinib-resistant colonies, indicating that ENU mutagenesis is beneficial in establishing an unbiased and robust cell-based resistance screen system of *KIT* gene.

The results of ENU mutagenesis followed by sunitinib selection were in concordance with the findings observed with sunitinib-resistant patients, defining D816 and D820 amino acids as the most vulnerable sites for acquired mutations within the KIT kinase activation loop. Similarly, imatinib selection identified T670, D816, and D820 as resistant mutation hotspots. The frequency of secondary mutations with sunitinib or imatinib selection with Ba/F3 KIT$^{502\text{-}3AYins}$ cells was quite low (Fig. 4). In contrast, clones carrying a juxtamembrane KIT$^{557\text{-}8WKdel}$ mutation had a significantly higher mutation rate. In keeping with these differences, previous biochemical studies revealed that tumors with KIT exon 9 mutation had less AKT activation than tumors with mutations of exon 11, suggesting that these KIT mutants may recruit different downstream substrates (22). The latter hypothesis may also explain the genotype-dependent response of GIST patients to different TKIs.

Recently, the crystal structure of the KIT ectodomain was characterized, showing that KIT dimerization is driven by bivalent binding of KIT ligand and stabilized by lateral D4-D4 and D5-D5 interactions of two neighboring KIT ectodomains (23). Activating oncogenic mutations reported thus far within the ectodomain of KIT map to the D5-D5 interface, which presumably stabilize receptor dimers and thus activate the kinase in the absence of ligand. In contrast, juxtamembrane domain mutations are thought to induce kinase activation by disrupting the autoinhibitory conformation of the juxtamembrane domain. The different mechanisms of activation of constitutive KIT kinase activity seen with different mutant oncoproteins may affect the mutation rates yielded from the mutagenesis screen. KIT exon 11 mutants largely rely on the structural changes conferred by secondary mutations to overcome inhibition of KIT kinase activity and with extracellular domain mutants similarly acquisition of secondary mutations that stabilize the active conformation of the KIT kinase is required. It is therefore not surprising that the spectrum of secondary mutations between the two mutant isoforms did not differ. Although both D816 and D820 do not interact directly with the inhibitors, the mutations at these sites affect the A-loop conformation as well as the overall conformation of the kinase (Fig. 5), preventing drug binding (19).

Unfortunately, comprehensive molecular studies are constrained by the low number of patients who are surgical candidates after failing two TKIs; thus, the tissue available for investigating mechanisms of resistance is limited. Taken together, the data obtained from clinical samples as well as from the *in vitro* mutagenesis screens suggest that sunitinib resistance shares similar pathogenetic mechanisms seen in imatinib failure, with acquisition of secondary mutations in the activation loop conferring resistance to both drugs. In contrast, the imatinib resistance screens showed a slightly higher mutation rate and a wider mutation spectrum, spanning both kinase domains. In addition, the *in vitro* resistance screens applied to either ectodomain or juxtamembrane domain KIT mutants suggest that the location of the primary mutation may trigger different mechanisms of drug resistance, with a higher rate of resistant mutations seen with primary KIT exon 11 mutants.

Disclosure of Potential Conflicts of Interest

R. DeMatteo, advisory board and honoraria, Novartis. R. Maki, research funding, Pfizer. The other authors reported no conflicts of interest.

Acknowledgments

We thank Kai Xu (Structural Biology Program, Sloan Kettering Institute), Diann DeSantis for clinical follow-up, and Milagros Soto for editorial support.

Published OnlineFirst October 27, 2009; DOI: 10.1158/1078-0432.CCR-09-1315

References

1. Blanke CD, Demetri GD, von Mehren M, et al. Long-term results from a randomized phase II trial of standard- versus higher-dose imatinib mesylate for patients with unresectable or metastatic gastrointestinal stromal tumors expressing KIT. J Clin Oncol 2008;26:620–5.
2. Heinrich MC, Corless CL, Demetri GD, et al. Kinase mutations and imatinib response in patients with metastatic gastrointestinal stromal tumor. J Clin Oncol 2003;21:4342–9.
3. Antonescu CR, Besmer P, Guo T, et al. Acquired resistance to imatinib in gastrointestinal stromal tumor occurs through secondary gene mutation. Clin Cancer Res 2005;11:4182–90.
4. Prenen H, Cools J, Mentens N, et al. Efficacy of the kinase inhibitor SU11248 against gastrointestinal stromal tumor mutants refractory to imatinib mesylate. Clin Cancer Res 2006;12:2622–7.
5. Russell WL, Kelly EM, Hunsicker PR, Bangham JW, Maddux SC, Phipps EL. Specific-locus test shows ethylnitrosourea to be the most potent mutagen in the mouse. Proc Natl Acad Sci U S A 1979;76:5818–9.
6. Antonescu CR, Sommer G, Sarran L, et al. Association of KIT exon 9 mutations with nongastric primary site and aggressive behavior: KIT mutation analysis and clinical correlates of 120 gastrointestinal stromal tumors. Clin Cancer Res 2003;9:3329–37.
7. Agaram NP, Laquaglia MP, Ustun B, et al. Molecular characterization of pediatric gastrointestinal stromal tumors. Clin Cancer Res 2008;14:3204–15.
8. Guo T, Agaram NP, Wong GC, et al. Sorafenib inhibits the imatinib-resistant KITT670I gatekeeper mutation in gastrointestinal stromal tumor. Clin Cancer Res 2007;13:4874–81.
9. Heinrich MC, Maki RG, Corless CL, et al. Primary and secondary kinase genotypes correlate with the biological and clinical activity of sunitinib in imatinib-resistant gastrointestinal stromal tumor. J Clin Oncol 2008;26:5352–9.
10. Hirota S, Isozaki K, Moriyama Y, et al. Gain-of-function mutations of c-kit in human gastrointestinal stromal tumors. Science 1998;279:577–80.
11. Heinrich MC, Corless CL, Duensing A, et al. PDGFRA activating mutations in gastrointestinal stromal tumors. Science 2003;299:708–10.
12. Rubin BP, Singer S, Tsao C, et al. KIT activation is a ubiquitous feature of gastrointestinal stromal tumors. Cancer Res 2001;61:8118–21.
13. Lasota J, Kopczynski J, Sarlomo-Rikala M, et al. KIT 1530ins6 mutation defines a subset of predominantly malignant gastrointestinal stromal tumors of intestinal origin. Hum Pathol 2003;34:1306–12.
14. Debiec-Rychter M, Sciot R, Le Cesne A, et al. KIT mutations and dose selection for imatinib in patients with advanced gastrointestinal stromal tumours. Eur J Cancer 2006;42:1093–103.
15. Demetri GD, van Oosterom AT, Garrett CR, et al. Efficacy and safety of sunitinib in patients with advanced gastrointestinal stromal tumour after failure of imatinib: a randomised controlled trial. Lancet 2006;368:1329–38.
16. Nishida T, Kanda T, Nishitani A, et al. Secondary mutations in the kinase domain of the KIT gene are predominant in imatinib-resistant gastrointestinal stromal tumor. Cancer Sci 2008;99:799–804.
17. Debiec-Rychter M, Cools J, Dumez H, et al. Mechanisms of resistance to imatinib mesylate in gastrointestinal stromal tumors and activity of the PKC412 inhibitor against imatinib-resistant mutants. Gastroenterology 2005;128:270–9.
18. Wardelmann E, Merkelbach-Bruse S, Pauls K, et al. Polyclonal evolution of multiple secondary KIT mutations in gastrointestinal stromal tumors under treatment with imatinib mesylate. Clin Cancer Res 2006;12:1743–9.
19. Gajiwala KS, Wu JC, Christensen J, et al. KIT kinase mutants show unique mechanisms of drug resistance to imatinib and sunitinib in gastrointestinal stromal tumor patients. Proc Natl Acad Sci U S A 2009;106:1542–7.
20. von Bubnoff N, Veach DR, van der Kuip H, et al. A cell-based screen for resistance of Bcr-Abl-positive leukemia identifies the mutation pattern for PD166326, an alternative Abl kinase inhibitor. Blood 2005;105:1652–9.
21. Bradeen HA, Eide CA, O'Hare T, et al. Comparison of imatinib mesylate, dasatinib (BMS-354825), and nilotinib (AMN107) in an *N*-ethyl-*N*-nitrosourea (ENU)-based mutagenesis screen: high efficacy of drug combinations. Blood 2006;108:2332–8.
22. Duensing A, Medeiros F, McConarty B, et al. Mechanisms of oncogenic KIT signal transduction in primary gastrointestinal stromal tumors (GISTs). Oncogene 2004;23:3999–4006.
23. Yuzawa S, Opatowsky Y, Zhang Z, Mandiyan V, Lax I, Schlessinger J. Structural basis for activation of the receptor tyrosine kinase KIT by stem cell factor. Cell 2007;130:323–34.
24. Liegl B, Kepten I, Le C, et al. Heterogeneity of kinase inhibitor resistance mechanisms in GIST. J Pathol 2008;216:64–74.

AACR American Association for Cancer Research

Clinical Cancer Research

Mechanisms of Sunitinib Resistance in Gastrointestinal Stromal Tumors Harboring *KIT*$^{AY502-3ins}$ Mutation: An *In vitro* Mutagenesis Screen for Drug Resistance

Tianhua Guo, Mihai Hajdu, Narasimhan P. Agaram, et al.

Clin Cancer Res 2009;15:6862-6870. Published OnlineFirst October 27, 2009.